Anti-fouling characteristics of surface-confined oligonucleotide strands bioconjugated on streptavidin platforms in the presence of nanomaterials

Mònica Mir [a,b,∗], Petra J. Cameron [c], Xinhua Zhong [d], Omar Azzaroni [a,e,∗], Marta Álvarez [a], Wolfgang Knoll [a]

[a] Max-Planck-Institut für Polymerforschung, Ackermannweg, 10, 55128 Mainz, Germany
[b] Nanobioengineering Group, Institute for Bioengineering of Catalonia (IBEC), Josep Samitier 1-5, 08028 Barcelona, Spain
[c] Department of Chemistry, University of Bath, Bath BA2 7AY, United Kingdom
[d] Department of Chemistry, East China University of Science and Technology, 200237 Shanghai, China
[e] INIFTA-CONICET-UNLP, C.C. 16 Suc. 4 (1900) La Plata, Argentina

ARTICLE INFO

ABSTRACT

This work describes our studies on the molecular design of interfacial architectures suitable for DNA sensing which could resist non-specific binding of nanomaterials commonly used as labels for amplifying biorecognition events. We observed that the non-specific binding of bio-nanomaterials to surface-confined oligonucleotide strands is highly dependent on the characteristics of the interfacial architecture. Thiolated double stranded oligonucleotide arrays assembled on Au surfaces evidence significant fouling in the presence of nanoparticles (NPs) at the nanomolar level. The non-specific interaction between the oligonucleotide strands and the nanomaterials can be sensitively minimized by introducing streptavidin (SAv) as an underlayer conjugated to the DNA arrays. The role of the SAv layer was attributed to the significant hydrophilic repulsion between the SAv-modified surface and the nanomaterials in close proximity to the interface, thus conferring outstanding anti-fouling characteristics to the interfacial architecture. These results provide a simple and straightforward strategy to overcome the limitations introduced by the non-specific binding of labels to achieve reliable detection of DNA-based biorecognition events.

© 2009 Elsevier B.V. All rights reserved.

1. Introduction

The fields of nanobiotechnology and nanomedicine are becoming increasingly important in research and industry. Within this growing research field, the ability to control the adsorption of biomolecules, nanomaterials and bio-inorganic hybrids to solid supports plays a key role in achieving reliable and competitive devices. For example, deposition of proteins, cells or bacteria on the surface of an implant or an *in vivo* biosensor usually leads to failure of these devices [1]. Health problems can be caused due to surface-fouling by microorganisms during the food preparation process. Electrochemical analysis is also affected by the adsorption of biomolecules on the surface, where the unwanted molecules result in the passivation of the electrode surface [2]. The diffusion of reagents in devices containing microfluidic circuits can change

drastically if the surface of the channels is affected by fouling [3]. The undesirable non-specific adsorption of different materials on surfaces must be eliminated in effective biosensors as it leads to a reduction in the sensitivity and specificity of the device. For applications such as biosensing, affinity chromatography, biocatalysis or microfluidics it is important not only to build a non-fouling surface, but also to have suitable recognition sites on the non-fouling surface in order to attach specific ligands with desired orientation and coverage, and to ensure a reproducible and reliable response. Thus, the molecular design of a biosensing platform that exhibits: (a) a reproducible and stable surface with resistance to non-specific binding and (b) good control over ligands immobilization is not a trivial task as is of high priority in biosensing community.

Within the great variety of biosensing platforms, of particular relevance is that one concerning to the detection of DNA hybridization. The most common interfacial architecture consists of monolayers of thiolated oligonucleotide probes assembled on gold surfaces forming a brush-like layer [4–6]. However, during last years the use of streptavidin (SAv) as an anchoring layer received increasing attention [7,8]. This is due to the fact that the SAv platform

---

∗ Corresponding author at: Institute for Bioengineering of Catalonia (IBEC), Josep Samitier 1-5, 08028 Barcelona, Spain.
E-mail address: mmir@ibec.pcb.ub.es (M. Mir).

enables an optimized distribution and spacing of the probe strands on the Au electrode, thus facilitating the hybridization process. Moreover, depending on the characteristics of the read out system, it is a common practice to use labeled-biomolecules, enzymes, fluorophores or nanoparticles (NPs) to enhance the detection of the biorecognition process [9].

Fluorescence-based transduction is probably one of the most sensitive strategies to detect DNA or oligonucleotide hybridization. Quantum dots (QDs) are nanomaterials that represent a very interesting type of fluorescent nanoparticles [10]. At present, they constitute the greatest promise as labels in fields like biosensing or biological imaging [10]. This is based on their remarkable photostability, high fluorescence yield, low rates of photobleaching and extinction coefficients comparable to conventional organic fluorophores, which render them outstanding candidates for fluorescent labeling of biomolecules. In spite of the widespread use of QDs combined with DNA in biosensing [11] and design of functional materials [12], little is known about the interaction and non-specific binding interactions between these nanomaterials and oligonucleotide strands at solid-liquid interfaces.

In this work we studied with particular emphasis the non-specific adsorption of QDs on surface-confined oligonucleotide strands formed by assembly of thiolated strands and by bioconjugation of biotinylated strands on SAv platforms. Our studies show notable differences between both platforms, indicating that the commonly used thiolated DNA assemblies are prone to non-specific binding of QDs. In contrast, the SAv-based did not evidence any non-specific adsorption of the nanomaterials. These results were also extended to the use of biomolecules, like streptavidin, as labels obtaining similar differences between both platforms.

2. Experimental

2.1. Materials

The oligonucleotide sequences; 18-mer thiol labeled capture probe (SH-C$_6$-5'-TTTTGTACATCACAACTA-3ĭ), 18-mer biotinylated capture probe (biotin-5'-TTTTGTACATCACAACTA-3ĭ) and 15-mer target (5'-TAGTTGTGATGTACA -3ĭ) used in this work were purchased from MWG Biotech AG. All stock oligonucleotide solutions were 100 μM prepared with milliQ water and stored at -20 °C. Streptavidin, mercaptoundecanol, 2-mercaptoethanol, phosphate buffered saline, polyethylene glycol sorbitan monolaurate (tween 20), trioctylphosphine (TOP), oleylamine, oleic acid, 1-octadecene (ODE), CdO, Se powder and 3-mercaptopropionic acid (MPA) were purchased from Sigma. Biotin-terminated thiol was obtained from Roche Diagnostics.

2.2. Synthesis of MPA-Capped CdSe nanoparticles

Oil-soluble CdSe nanoparticles were prepared according to a literature method [13]. Typically, 5.0 mL of oleylamine and 0.15 mL of Se stock solution (2.1 M in TOP) were loaded in a 50 mL three neck round-bottom flask, and the mixture was heated to 300 °C in a flow of argon. 1.0 mL of Cd stock solution (0.3 M, obtained by dissolving CdO in 6-fold of oleic acid and ODE at elevated temperature) was injected quickly into the reaction flask. The temperature was then set at 280 °C for the subsequent growth and annealing of nanocrystals. After completion of particle growth, the reaction mixture was allowed to cool to ~60 °C, and 10 mL of methanol was added. The obtained CdSe nanocrystals were precipitated by adding methanol into the toluene solution and further isolated and purified by repeated centrifugation and decantation. MPA-Capped water-soluble QDs were obtained by a ligand replacement reaction [14]. Due to the carboxylic group in the MPA

ligand, the obtained MPA-capped CdSe QDs are negative charged in aqueous solutions. The mean size of the CdSe QDs used for the following experiment is ~4.5 ± 0.3 nm with emission wavelength $\lambda = 620$ nm.

2.3. Biomolecules immobilization

Both interfacial architectures involving thiolated oligonucleotides (DNA-SH) and biotinylated oligonucleotides bioconjugated on SAv monolayers (DNA-SAv) were assembled onto gold surfaces. The DNA-SH architecture was prepared by incubating the gold films in a 1 μM solution of thiolated capture probe in 1 M KH$_2$PO$_4$ for 2 h, the slide then was placed in a 1 mM solution of mercaptoethanol in milliQ water for 1 h to backfill any empty spaces between the capture probe strands. It is worth mentioning that the backfilling also improves the orientation of the oligonucleotide strands leading to an improvement of the hybridization process.

The DNA-SAv architectures were constructed by chemisorbing a mixed self-assembled monolayer of 12-mercaptododecanoic-(-8-biotinoylamido-3,6-dioxaoctyl)amide and 11-mercapto-1-undecanol in ethanol in a 1:9 ratio [15]. Then, the biotinylated surface was incubated in a 1 μM streptavidin solution in 10 mM PBS, 100 mM NaCl at pH 7.4, leading to a compact monolayer evenly distributed on the Au surface [16,17]. Considering that SAv has unique properties as an adapter for the binding of a second layer of biotinylated molecules and the extremely high and very specific interaction with biotin ($K = 10^{15}$ L mol^{-1}), the resulting protein layer acts as stable platform for supramolecularly anchoring the biotinylated capture probes. Both surface architectures were hybridized with a 1 μM ss-DNA target solution and afterwards 1 μM solution of streptavidin or QDs respectively were left to interact with both platforms in order to investigate the effect of non-specific binding.

In both platforms, the unbounded molecules on the surface sensor were rinsed away after each immobilization step with the buffer used in the immobilization step.

2.4. Surface acoustic wave (SAW) measurements

The non-specific adsorption of SAv on both platforms was measured by acoustic wave sensor spectroscopy (SAW) (S-sens® k5, Nanofilm Surface Analysis). The sensor chip array consists of five gold sensors with a sensing area of 6.3 mm^2 each. The chips were cleaned before use by plasma treatment for 5 min at 300 W under argon atmosphere. All incubations were programmed and injection was done automatically at a flow rate of 20 μL min^{-1}. After each experiment an injection of 5% glycerol solution was required for calibration purposes [18].

2.5. Surface plasmon fluorescence spectroscopy (SPFS)

The binding of QDs on both interfacial architectures was monitored by surface plasmon fluorescence spectroscopy (SPFS) [19–21]. Laser light at $\lambda = 594.6$ nm was used to excite surface plasmons in the gold film (coupled in the Kretschmann configuration). The QDs located near the gold–dielectric interface can be excited by the surface plasmon that propagates along this interface. Photons emitted from the QDs were monitored with a photomultiplier. To avoid collection of scattered and transmitted laser light, a $\lambda = 611$ nm narrow band pass filter was placed in front of the photomultiplier. The sensor chip was a ~50 nm evaporated gold film on BK7 glass with ~2 nm of chromium being evaporated just prior to the gold deposition to improve adhesion between the gold and glass. All incubations were done at a flow rate of 20 μL min^{-1}.
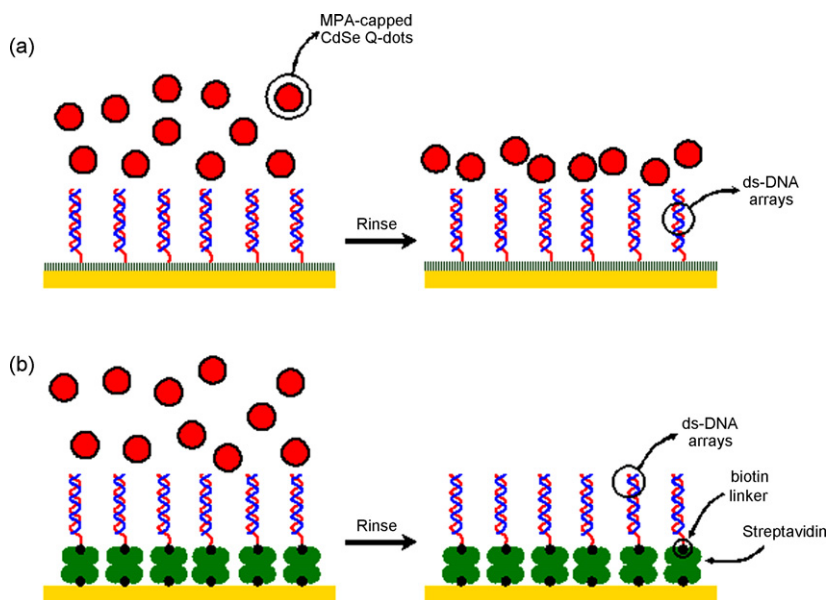
Fig. 1. . Simplified cartoon describing the interaction of the CdSe QDs with both interfacial architectures: (a) thiolated oligonucleotide strands, DNA-SH; (b) biotinylated oligonucleotide strands assembled on streptavidin platforms, DNA-SAv.

3. Results and discussion

Our experimental studies were carried out in two different interfacial architectures: (a) thiolated oligonucleotides (DNA-SH) and (b) biotinylated oligonucleotides bioconjugated on SAv monolayers (DNA-SAv) (Fig. 1).

The non-specific binding of QDs on both platforms was measured by SPFS. The binding curves in Fig. 2 display the striking differences between both interfacial architectures. The injection of the MPA-capped CdSe QDs into the SPFS chamber containing the DNA-SAv platform is evidenced as an increase in the fluorescence signal, $\sim1.5 \times 10^6$ cps. This is as a consequence of the excitation of the QDs in the surroundings of the solid–liquid interface [22]. The fluorescence signal was monitored over a period of 1 h displaying good stability after the injection. This fact indicates that the maximum concentration of QDs is achieved during the early stages of the immobilization and no significant changes in the population of QDs occur in the surroundings of the interface. Thereafter, the sensor surface was rinsed by flushing buffer solution through the SPFS chamber. Immediately, the fluorescence signal decayed to the original background signal obtained prior to injecting the
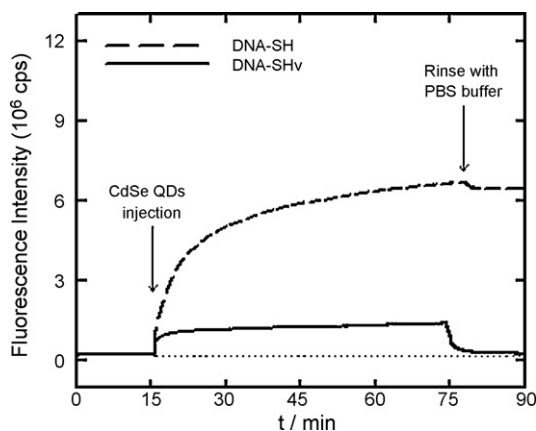

Fig. 2. . Surface plasmon fluorescence spectroscopy sensorgrams describing the binding of the CdSe QDs to the DNA-SH (dashed line) and DNA-SAv (solid line) platforms.

QDs-containing solution, thus giving a clear indication that the interfacial architecture is not fouled by the nanoparticles.

A different scenario was observed when the same experiment was repeated in the presence of the DNA-SH. After injecting the MPA-capped CdSe QDs into the SPR chamber, the fluorescence signal evidenced a continuous increase reaching values larger than those previously obtained in the presence of DNA-SAv, $\sim6.5 \times 10^6$ cps. Rinsing the sensor surface with buffer only promoted a slight change in the fluorescence signal, evidencing that most of the fluorescent nanomaterials remained at the interface, and consequently the sensor surface was heavily fouled by the CdSe QDs.

In principle, this experimental observation is counterintuitive. The hybridized oligonucleotide strands on the DNA-SH/Au platform represent a negatively charged interface where the phosphate groups are responsible for the anionic charges. The interaction with the negatively charged QDs should be repulsive, thus leading to a facile removal of the nanomaterials after rinsing. The experimental evidence indicates the opposite case, where the dominant interactions between the oligonucleotides and the nanoparticles are attractive. This observation is in line with recent results reported by Sandström et al. [23] working on the non-specific binding of citrate-stabilized Au nanoparticles to double stranded oligonucleotides. These authors reported a detailed study describing how negatively charged nanoparticles significantly bind non-specifically to double stranded DNA. Even if the non-specific binding of single-stranded oligonucleotides to Au nanoparticles has been reported by Mirkin and co-workers [24], the case involving double stranded oligonucleotides is a completely different scenario. Single stranded DNA binds non-specifically to flat Au surfaces and Au NPs by means of interactions provided by their bases. However, in the case of double stranded DNA these functional groups are not available for interacting with the nanomaterials. One explanation for this interesting phenomenon was proposed by Sandström et al. [23] suggesting that a possible mechanism could be ion-induced dipole dispersive interactions, where the negatively charged phosphate groups on the DNA induce dipoles in the highly polarizable NPs. This fact would explain why the CdSe QDs remain at a large extent on the sensor surface.

Another possible reason for the non specific adsorption of these negatively capped QDs on the negative DNA surface is the existence
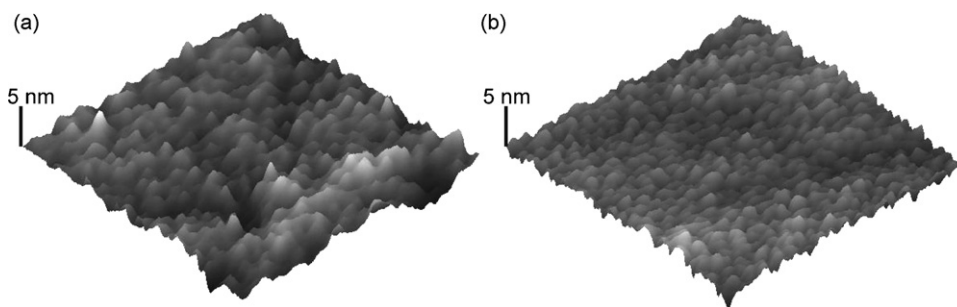
Fig. 3. . 500 μm × 500 μm AFM topography images for the DNA SAM (a) and SA SAM (b) platforms.

of holes in the DNA layer film, which allow the penetration of these molecules in lower charge repulsion areas. Previous studies carried out with these two sensor platforms showed a higher capture probe packing in the system with the DNA directly immobilised on the surface. In the DNA SAM configuration a surface coverage of 0.05 mol mm^{-2} was reported, while in the SA SAM configuration lower capture probe coverage of 0.035 mol mm^{-2} was detected. However, the number of target molecules hybridised in the SA SAM system is higher comparing with the hybridisation in the DNA SAM platform. The lower hybridization efficiency of the DNA SAM platform was explained as a consequence of the high capture probe density in this system, which hindrance the access of the target to the probe [25]. These results show a highly packed DNA SAM platform, where is improbable to find holes on the film. In order to assure the lack of defects on both platforms, where the molecules could non specifically be adsorbed, surface topographic studies of both platforms were carried out with AFM. Simultaneous tapping mode topographic and phase imaging were carried out on modified gold mica substrates. Different distribution of the biomolecules on the surface was observed by comparing the phase images of both systems (Fig. 3). However, in both surfaces no holes were observed on the film, showing uniform and homogeneous distribution of the biomolecules on the surface.

On the other hand, we also observed that double stranded oligonucleotide brushes presenting SAv as an underlying platform describe a completely different interfacial behavior, i.e. no binding is observed. Considering the similarities and differences between both platforms it is plausible to ascribe these non-fouling characteristics to the presence of SAv in the interfacial architecture. Recently, van Oss and co-workers [26] discussed the macroscopic-scale surface properties of SAv and their influence on the non-specific interactions with biopolymers. The use of SAv-coated glass substrates presenting a high surface hydrophobicity prevented the fouling of biomolecules like immunoglobulins (IgG) or human serum albumin (HSA). The hydrophilic repulsion between the planar SAv-coated surface and the IgG or HSA precluded the non-specific binding to the surface, to which biotinylated molecules can be easily and firmly attached. In accordance to van Oss et al., this anti-fouling behavior is governed by (non-electrostatic) polar macroscopic-scale hydrophilic repulsion between the SAv-coated surface and the biomolecules. In our case, the SAv underlayer would confer similar properties to the interfacial architecture, where a strong hydrophilic repulsion would prevent the non-specific binding of the nanomaterials.

To further extend of use of the SAv underlayer in DNA sensing platforms we studied the interfacial behavior of SAv molecules in solution interacting with DNA-SH and DNA-SAv. The reason for choosing SAv interacting with the different sensor architectures lies in the fact that it is commonly used as a linker for labeling biotinylated oligonucleotides [27–29] and, in some cases, it has been reported that it non-specifically binds to different substrates [30]. These interfacial studies were carried out using an acous-

tic waveguide device (SAW) [31–34]. The principle of operation of SAW is based on an electric potential applied to a piezoelectric substrate via interdigitated transducers which creates a surface-localized acoustic wave. The phase and amplitude of the surface wave are monitored with time through electrical connections to the output transducers. All sensing occurs within an interfacial region where significant acoustic displacement is detected. This is given by the thickness of the penetration depth which is a function of the viscosity of the surface medium and operating frequency of the device. In particular, phase response is very sensitive to both mass and viscoelastic properties and is commonly the parameter of choice for monitoring the immobilization of biomolecules [35].

Fig. 4 shows the SAW sensorgrams for 1 μM SAv in contact with both interfacial architectures forming brush-like oligonucleotide assemblies at the solid-liquid interface. The DNA-SH assembly described a sudden increase in phase signal after injecting the SAv solution into the chamber. After 10 min the sensor surface was flushed with PBS buffer and the SAW device monitored only a slight decrease in phase signal. This fact evidences that the proteins remain in the surroundings of the interfacial region (within the penetration depth) where the SAW detects their presence. In other words, the DNA-SH interface is sensitively fouled in contact with the proteins.

The same experiment with the DNA-SAv sensor displayed a significant increase in phase signal, larger that in the case of DNA-SH. This could be attributed to the fact that the DNA-SAv sensor presents an interfacial architecture that could be more sensitive to interfacial viscoelastic changes. Phase changes are extremely sensitive to viscous water and mass loading, which are determined by the characteristics of the interfacial architecture [31].

After rinsing with buffer the phase values returned to approximately the original background signal obtained before injecting the
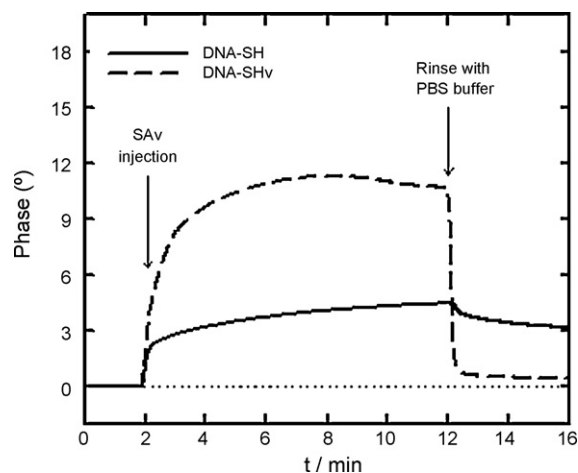

Fig. 4. . Phase response of the surface acoustic wave device monitoring the binding of the CdSe QDs to the DNA-SAv (dotted line) and DNA-SH (solid line) platforms.

SAv solution, thus indicating that the DNA-SAv sensor surface was not fouled by the biomolecules. These results are in agreement with the experimental results obtained working with negatively charged QDs where the presence of the SAv underlayer confers outstanding non-fouling properties to the sensor surface.

4. Conclusions

The goal of our work was to investigate new strategies for designing DNA sensing interfaces which could resist non-specific binding of bio-nanomaterials commonly used as labels. These results evidence the key role played by the SAv underlayer in the creation of interfacial architectures capable of minimizing the non-specific binding of negatively charged nanoparticles and streptavidin. The main role attributed to the SAv layer lies in the significant polar hydrophilic repulsion between the SAv-modifided surface and the nanomaterials in solution, which confers the interface anti-fouling characteristics. In many cases, oligonucleotide brushes were assembled onto SAv platforms with the aim of controlling the grafting density and interspacing between DNA strands. This led to the creation of highly reproducible interfaces displaying rapid hybridization kinetics in comparison to thiolated DNA brushes [35]. The experimental evidence discussed in this work adds another key advantage of using SAv-based DNA platforms, which relies on their capabilities to strongly resist the non-specific binding of labeling materials. The different fouling characteristics of DNA-SAv and DNA-SH interfacial architectures is an important aspect that should be taken into account when choosing a platform for biosensing applications.

Acknowledgements

References

[1] W. Reichert, A. Sharkawy, in: A. Von Recum (Ed.), Handbook of Biomaterials Evaluation, Taylor & Francis, Washington D.C., 1999, p. 439.
[2] M. Kyrolainen, S.M. Reddy, P.M. Vadgama, Anal. Chim. Acta 353 (1997) 2813.
[3] S. Woodward, Diabetes Care 5 (1982) 278.
[4] M. Mir, I. Katakis, Mol. Biosys. 3 (2007) 620.
[5] (a) M. Cardenas, J. Barauskas, K. Schillen, J.L. Brennan, M. Brust, T. Nylander, Langmuir 22 (2006) 3294;
(b) H. Kimura-Suda, D.Y. Petrovykh, M.J. Tarlov, L.J. Whitman, J. Am. Chem. Soc. 125 (2003) 9014.
[6] M. Mir, I. Katakis, Talanta 75 (2008) 432.
[7] C.L. Smith, J.S. Milea, G.H. Nguyen, Top. Curr. Chem. 261 (2006) 63.
[8] W. Knoll, M. Liley, D. Piscevic, J. Spinke, M.J. Tarlov, Adv. Biophys. 34 (1997) 231.
[9] I. Willner, E. Katz (Eds.), Angew. Chem. Int. 43 (2004) 6042.
[10] (a) S.K. Shin, H.J. Yoon, Y.J. Jung, J.W. Park, Curr. Opin. Chem. Biol. 10 (2006) 423;
(b) A.P. Alivisatos, W. Gu, C. Larabell, Annu. Rev. Biomed. Eng. 7 (2005) 55;
(c) L. Pasquato, P. Pengo, P. Scrimin, Nanoparticles, Building Blocks for Nanotechnology, Springer Science, New York, 2004, p. 251 (Chapter 10);
(d) M. Murcia, C.A. Naumann, Biofunctionalization of Nanomaterial, Wiley-VCh, Weinheim, 2005, p. 15 (Chapter 1).
[11] (a) J. Wang, Small 1 (2005) 1036;
(b) J. Wang, G. Liu, A. Merkoci, J. Am. Chem. Soc. 125 (2003) 3214;
(c) E. Katz, I. Willner, Nanobiotechnology, VCH-Wiley, Weinheim, 2004, p. 200 (Chapter 14).
[12] (a) R. Gill, F. Patolsky, E. Katz, I. Willner (Eds.), Angew. Chem. Int. 44 (2005) 4554;
(b) R. Freeman, R. Gill, M. Beissenhirtz, I. Willner, Photochem. Photobiol. Sci. 6 (2007) 416.
[13] X. Zhong, Y. Feng, Y. Zhang, J. Phys. Chem. C 111 (2007) 526.
[14] W.C.W. Chan, S. Nie, Science 281 (1998) 2016.
[15] J. Spinke, M. Liley, F.J. Schmitt, H.J. Guder, L. Angermaier, W. Knoll, J. Chem. Phys. 99 (1993) 7012.
[16] O. Azzaroni, M. Mir, W. Knoll, J. Phys. Chem. B 111 (2007) 13499.
[17] O. Azzaroni, M. Mir, M. Alvarez, L. Tiefenauer, W. Knoll, Langmuir 24 (2008) 2878.
[18] K. Saha, F. Bender, A. Rasmusson, E. Gizeli, Langmuir 19 (2003) 1304.
[19] S. Ekgasit, G. Stengel, W. Knoll, Anal. Chem. 76 (2004) 4747.
[20] S. Ekgasit, F. Yu, W. Knoll, Langmuir 21 (2005) 4077.
[21] T. Neumann, M.L. Johansson, D. Kambhampati, W. Knoll, Adv. Funct. Mater. 12 (2002) 575.
[22] S. Joseph, T.M.M. Gronewold, M.D. Schlensog, C. Olbrich, E. Quandt, M. Famulok, M. Schirner, Biosens. Bioelectron. 20 (2005) 1829.
[23] P. Sandström, M. Boncheva, B. Akerman, Langmuir 19 (2003) 7537.
[24] J.J. Storhoff, R. Elghanian, C.A. Mirkin, R.L. Letsinger, Langmuir 18 (2002) 6666.
[25] M. Mir, M. Alvarez, O. Azzaroni, W. Knoll, Langmuir 24 (2008) 13001.
[26] C.J. Van Oss, R.F. Giese, P.M. Bronson, A. Docoslis, P. Edwards, W.T. Ruyechan, Colloids Surf. B 30 (2003) 25.
[27] J. Liu, S. Tian, L. Tiefenauer, P.E. Nielsen, W. Knoll, Anal. Chem. 77 (2005) 2756.
[28] J. Wang, J. Li, A.J. Baca, J. Hu, F. Zhou, Y. Wan, D.W. Pang, Anal. Chem. 75 (2003) 3941.
[29] F. Lucarelli, G. Marrazza, M. Mascini, Langmuir 22 (2006) 4305.
[30] M.J.W. Ludden, A. Mulder, R. Tampe, D.N. Reinhoudt, J. Huskens (Eds.), Angew. Chem. Int. 46 (2007) 4104.
[31] E. Gizeli, Anal. Chem. 72 (2000) 5967.
[32] M.D. Schlensog, T.M.A. Gronewold, M. Tewes, M. Famulok, E. Quandt, Sens. Actuators B 101 (2004) 308.
[33] T.A.M. Gronewold, A. Baumgartner, E. Quandt, M. Famulok, Anal. Chem. 78 (2006) 4865.
[34] E. Gizeli, Biomolecular Sensors, Taylor & Francis, London, 2002, p. 176 (Chapter 7).
[35] X. Su, Y.J. Wu, W. Knoll, Biosens. Bioelectron. 21 (2005) 719.